The Effect of Thermal Loadings on the Dynamic Behavior of Cylindrical – Conical Intersection shell

Muhsan J. Jweeg[*] , Ammar A. Al-Filfily[**] & Ali B. Assi[***]

Received on: 28/8/2005
Accepted on: 1/6/2006

Abstract

This paper presented a numerical methods based on FEM were used to study the effect of temperature on the dynamic characteristic of composite cylindrical conical shell with different cone angle and wall thickness. The study taken into account the effect of temperature on the material properties of the selected material and the effect of pre stressing on the natural frequency of the shell. A general conclusions could be obtained from the static analysis ,i.e. for higher circumferential wave number, the effect of increasing the thickness is to produce higher natural frequencies. The natural frequency of the system may drops by about (12 %) as a result of the degeneration of the material properties due to temperature elevation. The higher circumferential wave number, the more pronounced is the influence of ply orientation on the resulting natural frequency changing the ply orientation for 0/90/0 to 75/-75/75 may increase the natural frequency by about (100 %). Finally the transient dynamic stresses may exceeds the design stress by a bout (50 %).

Keywords: composite shell; finite element method; vibration.

تأثير الاحمال الحرارية على الخواص الديناميكية للقشريات ذات الاتصال الاسطواني - المخروطي

الخلاصة

خلال هذا البحث تم بناء نموذج عددي لدراسة التاثير الحراري للخواص الديناميكية للقشور المحتوية على ربط اسطواني مخروطي والتي يكون فيها السمك متغير ولمختلف زواويا المخروط.

اظهر التحليل الديناميكي إن الترددات العالية كانت تقترن بسعات عالية مقارنة بالترددات الواطئة. أدت الزيادة في السمك إلى إنتاج ترددات طبيعية أعلى في حالة الأعداد الموجية المحيطية العالية. انخفضت الترددات الطبيعية للنظام بحوالي (12 %) نتيجة لتغير خواص المواد مع ارتفاع درجات الحرارة كما واظهر التحليل الديناميكي ان الترددات الطبيعية تختلف باختلاف زوايا لف كل طبقة بحيث تضاعفت قيمة التردد الطبيعي عند تغيير زاوية اللف من (0/90/0) الى (75/-75/75). وأخيرا كانت الأجهادات الديناميكية المرحلية تتجاوز الاجهادات التصميمية بحوالي (50 %) .

*** College of Engineering, AL-NAHREEN University/Baghdad**
****Technical College, Foundation of Technical Education /Baghdad**
***** Ministry of Science and Technology/Baghdad**

Introduction

The vibration of circular cylindrical and conical shells is of interest in a number of different fields including ocean engineering aeronautical engineering and civil engineering.

A knowledge of the free vibration characteristic of elastic shells is so important to the general understanding of the fundamental behavior of shells and to the industrial applications of these structures. In connection with the latter, the natural frequencies of the shell must be known in order to avoid the destructive effects of resonance associated with rotating or oscillating equipment or that arising from dynamic excitations such as earthquakes. The designing of a structure to isolate it from the destructive effects of resonant vibration, rather than strengthening it to withstand the vibration, is a recognized fact. This is achieved by elevating the natural frequencies of the structure so that they are sufficiently higher than the frequencies of the possible dynamic excitation in the vicinity.

The response of structures subjected to thermal environments is affected by the development of thermal stresses and by the deterioration of the materials of construction. The effect of temperature on the modulus of elasticity is far from being negligible to aircraft and rocket designers, for instance, because for such materials as titanium alloys, the modulus of elasticity may be at half of its room temperature value when subjected to a temperature rise of about 500 ^{o}C [1]. Other materials are also affected, and experimental investigations have shown linear relation, for most engineering materials, was predicted between modulus of elasticity and temperatures [2].

Ross C. T. [4] produced an elemental mass matrices for the vibration of conical and cylindrical shells, based on a semi-analytical approach. Frequencies and modes of vibration have been compared with existing solutions, and also with experimental results obtained from other literatures while Y. Takeuti, R. Ishida and Y. Tanigawa [8] presented a general treatment of the transient thermal stresses of a finite circular cylinder with consideration of the thermomechanical coupling effect using a new analytical technique. The transient response of the combustion chamber subjected to instantaneous pressure rise was studied by Osman M. A. [9] useing the F.E.M. Two solid rocket motors are considered as case studies. He obtained the maximum dynamic stresses and calculated the dynamic load factor .

Stiffness and mass formulation

Each element [3] ,as a matter of fact, is a truncated conical shell with two end nodes and four degrees of freedom per node (u, v, w, and θ) as shown in Fig. (1), therefore , each element has a total of eight degrees of freedom as a whole.

Since many of these degrees of freedom are not normally needed to define the mode shape, the u, v, and θ displacements were eliminated at all nodes, except the last one to save computational time and space in inverting the stiffness matrix and solving the eigenvalue equation. Therefore, the meridional mode shape was defined predominantly by the "w" displacements only.

This reduction process was given by Irons[5], its use enabled the program to reduce the sizes of the stiffness and mass matrices by a factor of about four.

The resulting mode of vibration is asymmetric, the circumferential shape being of lobar form, as shown in Fig.(2). In the meridional direction, the mode shapes depend on the geometry of the structure and also on the boundary conditions.

The vector of strains for a doubly-curved axisymmetric element was given by Novozhilor [6] which is;

$$\{\varepsilon\}=\begin{Bmatrix}\varepsilon_s\\ \varepsilon_\theta\\ \varepsilon_{s\theta}\\ \chi_s\\ \chi_\theta\\ \chi_{s\theta}\end{Bmatrix} \quad (1)$$

$$\varepsilon_s=\frac{1}{R_1\alpha}\frac{\partial u}{\partial \xi}+\frac{w}{R_1} \quad (2)$$

$$\varepsilon_\theta=\frac{1}{r}\left(\frac{\partial v}{\partial \theta}+u\sin\beta+w\cos\beta\right) \quad (3)$$

$$\varepsilon_{s\theta}=\frac{1}{r}\left(\frac{r}{R_1\alpha}\frac{\partial v}{\partial \xi}-\upsilon\sin\beta+\frac{\partial u}{\partial \theta}\right) \quad (4)$$

$$\chi_s=\frac{-1}{R_1^2\alpha^2}\frac{\partial^2 w}{\partial \xi^2}-u\frac{\partial^2\beta}{\partial s^2}+\frac{1}{R_1^2\alpha}\frac{\partial u}{\partial \phi} \quad (5)$$

$$\chi_\theta=-\frac{1}{r}\left(\frac{1}{r}\frac{\partial^2 w}{\partial\theta^2}-\frac{\cos\beta}{r}\frac{\partial v}{\partial\theta}+\frac{1}{R_1}\left(\frac{1}{\alpha}\frac{\partial w}{\partial\xi}-u\right)\sin\beta\right) \quad (6)$$

$$\chi_{s\theta}=\frac{2}{r}\left(-\frac{1}{R_1\alpha}\frac{\partial^2 w}{\partial\xi\partial\theta}+\frac{\sin\beta}{r}\frac{\partial w}{\partial\theta}+\frac{\cos\beta}{R_1\alpha}\frac{\partial v}{\partial\xi}-\frac{\sin\beta\cos\beta}{r}v-\frac{1}{R_1}\frac{\partial u}{\partial\theta}\right) \quad (7)$$

The assumed displacement functions were ;

$$u=\frac{(1-\xi)}{2}u_1\cos n\phi+\frac{(1+\xi)}{2}u_2\cos n\phi \quad (8)$$

$$v=\frac{(1-\xi)}{2}u_i\sin n\phi+\frac{(1+\xi)}{2}u_j\sin n\phi \quad (9)$$

$$w=\frac{(x^3-3x+2)}{4}w_1\cos nf+\frac{(1+x)(1-x)^2}{4}R_1aq_2\cos nf+\frac{(-x^3+3x+2)}{4}w_2\cos nf-\frac{(1-x)(1+x)^2}{4}R_1aq_2\cos nf \quad (10)$$

Or, in matrix form,

$$\begin{Bmatrix}u\\ v\\ w\end{Bmatrix}=[N]\{u_i\} \quad (11)$$

Where

$\{u_i\}$ = a matrix of nodal displacement

$[N]$ = a matrix of "shape function"

These displacement functions assume a linear variation of u and v with respect to the meridian of the shell. They are also allowed for a sinusoidal distribution in the circumferential direction to cater for the lobes of Fig.(2).

Hence, [N] matrix can be obtain

$$N=\begin{bmatrix}N_{11}&0&0&0&N_{15}&0&0&0\\ 0&N_{22}&0&0&0&N_{26}&0&0\\ 0&0&N_{33}&N_{34}&0&0&N_{37}&N_{38}\end{bmatrix} \quad (12)$$

where;

$$N_{11}=\frac{1-\xi}{2}\cos n\phi \quad N_{15}=\frac{1+\xi}{2}\cos n\phi$$

$$N_{22}=\frac{1-\xi}{2}\cos n\phi$$
$$N_{26}=\frac{1+\xi}{2}\cos n\phi \qquad (13)$$

$$N_{33}=\frac{\left(\xi^3-3\xi+2\right)}{4}$$
$$N_{37}=\frac{\left(-\xi^3+3\xi+2\right)}{4}\cos n\phi$$

$$N_{34}=\frac{(1+\xi)(1-\xi)^2 R_1\alpha}{4}\cos n\phi$$
$$N_{38}=\frac{-(1-\xi)(1+\xi)^2 R_1\alpha}{4}\cos n\phi$$

Substitution of the displacement function and its derivatives into the strain relationships, results the [B] matrix.

The stiffness matrix is given by:

$$[K]=\iint\begin{Bmatrix}BE\\BB\end{Bmatrix}^T\begin{bmatrix}A & B\\B & D\end{bmatrix}\begin{Bmatrix}BE\\BB\end{Bmatrix}dx\,dy$$

$$=\int_{-1}^{1}\int_{0}^{2\pi}\begin{Bmatrix}BE\\BB\end{Bmatrix}^T\begin{bmatrix}A & B\\B & D\end{bmatrix}\begin{Bmatrix}BE\\BB\end{Bmatrix}r\,d\phi\,R_1\,\alpha\,d\xi \qquad (14)$$

$$[K]=\pi R_1\alpha\int_{-1}^{1}\begin{Bmatrix}BE\\BB\end{Bmatrix}^T\begin{bmatrix}A & B\\B & D\end{bmatrix}\begin{Bmatrix}BE\\BB\end{Bmatrix}d\xi \qquad (15)$$

The mass matrix is given by;

$$[m]=\iint[N]^T\rho[N]t\,r\,d\phi\,R_1\alpha\,d\xi \qquad (16)$$

$$[m]=\pi R_1\alpha\rho\int_{-1}^{1}t\,r\,[N]^T[N]\,d\xi \qquad (17)$$

In global coordinates, the local matrices were converted to ;

$$[K]^o=[DC]^T[K][DC] \qquad (18)$$

and;

$$[m]^o=[DC]^T[m][DC] \qquad (19)$$

where;

$$[DC]=\begin{bmatrix}\zeta_1 & 0_4\\0_4 & \zeta_2\end{bmatrix}$$

$$\zeta_1=\begin{bmatrix}\cos\beta_1 & 0 & \sin\beta_1 & 0\\0 & 1 & 0 & 0\\-\sin\beta_1 & 0 & \cos\beta_1 & 0\\0 & 0 & 0 & 1\end{bmatrix},$$

$$\zeta_2=\begin{bmatrix}\cos\beta_2 & 0 & \sin\beta_2 & 0\\0 & 1 & 0 & 0\\-\sin\beta_2 & 0 & \cos\beta_2 & 0\\0 & 0 & 0 & 1\end{bmatrix}$$

Evaluation of natural frequencies

For free vibration, without damping, the equation of total energy is [3];

$$\Pi_P=\int_{vol}\frac{\{s\}^T\{e\}}{2}d(vol)-\{u_i\}^T\{P_i\}+\frac{\{\dot{u}_i\}^T[m]\{\dot{u}_i\}}{2} \qquad (20)$$

where

$\{\dot{u}_i\}$=a vector of nodal velocities

Assuming simple harmonic matrix take place, then

$u=A\sin(\omega t)$ (21)

and the velocity

$\dot{u}=\omega i\,A\cos(\omega t)$ (22)

Substituting (22) into (20)

$$\Pi_P=\int_{vol}\frac{\{\sigma\}^T\{\varepsilon\}}{2}d(vol)-\{u_i\}^T\{P_i\}-\frac{\omega^2}{2}\{u_i\}^T[m] \qquad (23)$$

Differentiating (23) with respect to {ui} and setting the derivative to zero, the following is obtained;

$\{P_i\}=[K]\{u_i\}-\omega^2[m]\{u_i\}$ (24)

where; {Pi} is a time dependent forcing vector

For free vibrations,{Pi}=0

Hence (24) becomes

$$\left|[K]-\omega^2[m]\right|=0 \quad (25)$$

or for the entire structure;

$$\left|[K]-\omega^2[M]\right|=0 \quad (26)$$

where, [M]=∑[m]=The mass matrix for the entire structure

After solving eqn.(26), all the natural frequencies and mode shapes would be known.

Dynamic characteristics under thermal loading

In view of the importance of the effect of thermal loading, especially in nuclear and aeronautical structural design, it would appear that there exists a need for more attention to be devoted to the effect of such loading upon the vibration of shells. Leissa [7] indicated that when considering the effect of thermal loading, two aspects have to be considered: namely, (a) the effect of the pre-stressing due to the temperature gradients, and (b) the effect of property variation with temperature.

For the case, in which the shell is subjected to some form of in-plane pre-stressing, a geometric stiffness matrix [Kg], describing the constitutive relationship between the force and displacement vectors as a result of the in-plane stressing, and in the absence of flexural effects, must be developed. Subsequently, the flexural and geometric stiffness matrices are summed to form the total stiffness matrix [kT] for each element : i.e

[KT]=[Kf]+[Kg] (27)

and the natural frequency can be obtained from :

$$\left|[K]_T-\omega^2[m]\right|=0 \quad (28)$$

The effect of property variation with temperature on the dynamic characteristic is taken into account by letting the modulus of elasticity to vary linearly with the temperature. Thus

E = Eo - ςEoT (29)

where Eo is the modulus of elasticity at room temperature

ς is the imperial coefficient dependent on the material

The pressure – time curve

The pressure behavior with time of burning of the solid propellant grain gives full information about internal processes inside the combustion chamber, and the time dependent load effect on the case of combustion chamber.

The differential equations that can describe the behavior of pressure – time curve, can be solved by internal ballistic of solid propellant charge should be take into consideration. For solving this task, it is important to know the type of solid propellant used.

The pressure time curve for the real rocket motor taken from the special document.

Results

A diverging conical – cylindrical intersection case was selected as a verification case for the dynamic analysis program because there is an available experimental data regarding the dynamic characteristic.

The geometrical and material properties of the case is shown in Fig.(3).

Table (1) represents a comparison of the natural frequencies, between the developed program, ANSYS and the available experimental data. The results agree very well with the experimental data.

The size and number of elements influence directly the accuracy of the results. However, if the number of elements is increased beyond a certain limit, the accuracy will not be improved by any significant amount. The F.E. convergence study for the selected combustion chamber, for the dynamic F.E. programs, are given in tables (2).

A plot of the convergence study for the two cases were also shown in Figs.(6.5) , (6.6) and (6.7).

CASE 1 COMBUSTION CHAMBER SHELL

A detailed study was performed on real case of rocket combustion chamber practical case because of its importance. The geometry and material properties was shown in Fig.(6).

A dynamic analysis was made to the real case of rocket combustion chamber case with the presence and absence of the effect of thermal loading. When there is no thermal loading, The dynamic characteristic was presented in tables from (3) to (5), each table presence dynamic characteristic of a different shell thickness and two different materials. The mode shapes which corresponding to thickness of (0.5 mm) and different lobe number plotted in figures from (7) to (12), each lobe number is associated with three different frequencies.

Then, the behavior of the rocket combustion chamber was examined under different thermal loading level, corresponding to temperature range from (0 – 500) Co for two different materials. The predicted dynamic characteristic was given in table (6) in which the material properties were taken to be temperature dependent. Another important effect of thermal loading on the dynamic characteristic was the effect of pre-stressing . The result of studying this effect was presented in tables from (7) to (12) for two different material and six lobe numbers. Some of the result of this table is plotted in Figs.(13) and (14).

Finally the transient behavior of the rocket combustion chamber is considered with different damping ratios and the results are shown in figures from (15) to (20).

CASE 2 Cylindrical – Conical Intersection Shell

A dynamic analysis was made to the cylindrical – conical shell case with and without presence of the effect of thermal loading, the dynamic characteristic was presented in tables from (13) to (16), each table presence dynamic characteristic of a different cone angle and different fiber orientation.

Then, Material 3 is used to study the effect of temperature on the dynamic characteristic of the cylindrical conical shell corresponding to temperature range from (20 -300) oC for three different cone angle. The resulting natural frequency variation with temperature is shown in figures from (21) to (26).

Discussion

Case 1

A dynamic analysis was performed on a thermally unloaded utilizing F.E. computer program Zimer – D. When the structure deformed in axi-symmetrical mode

shape with frequency of about (88 Hz) , the resulting amplitude is nearly null as shown in Fig.(7). While for higher frequency, there is appreciable amplitude occur with a down spike at the first cylindrical conical interface and another sharp edge at the second cylindrical conical interface as shown in figures (8) and (9).

The cantilever mode shape, in contrast to the first mode shape, appeared to has lower frequencies and higher amplitude as shown in figures from (10) to (12) for the first three consequent natural frequencies.

The higher the circumferential wave number, the more pronounced is the influence of thickness on the resulting natural frequency as shown in tables from (3) to (5).

For higher circumferential wave number, increasing the thickness by (50%) may double the natural frequency. This ratios may even increases for different materials as shown in tables (3) and (5).

As indicated by Lessia [7] , that the effect of thermal loading has two major aspect, the effect of property with temperature and effect of pre-stressing . The result of considering the first case, namely the effect of thermal loading on the structure dynamic response when the material property is allowed to vary with temperature, is presented in table (6).

Table 6 shows that the modulus of elasticity drops significantly (by about (30 %) in the working temperature change [8]. As a consequence, the natural frequency of the system drops by about (12). The effect of thermal pre-stressing on the dynamic response of the structure is presented in tables from (7) to (12). For the axisymmetric mode shape, the effect of thermal loading has appeared to have appreciable variable with temperature for lower frequencies as shown in Fig.(13), and this effect decays gradually with the influence of frequency.

The effect of changing the material on the dynamic response increases with higher frequencies.

In cantilever mode shape show no significant variation of natural frequency with temperature , but the material selection effect is qualitatively the same as shown in Fig.(14).

The transient analysis of the rocket combustion chamber is presented in figures from (15) to (20) for different damping ratio to explore the effect of this parameter on the dynamic behavior of the structure. When there is no damping at all, the response has persistent fluctuating deformation as shown in Fig.(15). Even this case is not partially happen ,but it was included for the sake of comparison. The more probable response is happen when the structure has under damped behavior as shown in Fig.(16). The critical instances of the structure is at the beginning of the combustion, when the pressure suddenly rises leading to over stressing the structure.

The effect of increasing the damping coefficient on the dynamic response of the structure is shown in figures from (17) and (18). The resulting transient stress are shown in figures from (19) to (20).

The under damped case, as expected the dynamic stresses exceeds the design stresses by about (50 %),hence these stresses are considered the more important in the design process.

Case 2

The results obtained in the present study are noted for the following features:

- **Effect of Cone Angle**

It was shown that a cone angle has a significant effect on the natural frequencies of a composite cylindrical – conical intersection shell. Considering composite shells produced of the same materials properties but different cone angle , it was found, for specific examples of table (14), that at ply orientation 35/-35/35 the natural frequency lowest by a factor (9%) and (22%) for cone angle 55o and 75o respectively. This result should not be viewed at as an upper limit, expressing the efficiency of lamination, but rather as a fine indication of the potential of composites in achieving an optimized design.

- **Frequency Dependence on the Number of Circumferential Waves (n)**

The variation of the first natural frequencies with n for three different composite materials are arranged in tables from (14) to (16).

The higher circumferential wave number, the more pronounced is the influence of ply orientation on the resulting natural frequency. For higher circumferential wave number, changing the ply orientation for 0/90/0 to 75/-75/75 may increase the natural frequency by about (100 %).

The frequency decrease as n is increased and a minimum is reached, then ω increases with n. The frequency first reaches a local maximum before dropping to a minimum value. The ratio of ωmax/ωmin for cone angle 35o and different ply orientation are (6.67 for 0/90/0, 4.44 for 35/-35/35, 3.89 for 55/-55/55 and 3.33 for 75/-75/5-75). A study of the parameters affecting the frequency distribution for various circumferential wave numbers seems to be worthwhile.

The effect of increasing circumferential wave number on the natural frequency for different material properties is study. As expected the natural frequency for material number (2) is higher than for material number (1) since the stiffness matrix for material (1) is lower than for material (2).

- **Effect of Temperature**

The effect of thermal loading on the structure dynamic response when the material property is allowed to vary with temperature, is presented in figures from (21) to (26).

Figure (21) shows that the natural frequency drops appreciably (by about 18 %) as the temperature change from (20 ^{o}C) to (300 ^{o}C) for axi-symmetrical mode shape. This ratio is decrease to about (16 %) and (13 %) for cone angle (55 ^{o}) and (75 o) respectively as shown in figures (22) and (23).

The effect of increasing cone angle in the case of constant thermal loading is presented in figures from (24) to (26).

Conclusion

The cantilever mode shape has lower frequencies and higher amplitude than the first mode shape.

For higher circumferential wave number increasing the thickness by (50 %) may double the resulting natural frequency.

The natural frequency of the system may drops by about (12 %) as a result of the degeneration of the material property due to temperature elevation.

The cantilever mode shape shows little effect with temperature than the axisymmetric mode shape when the material is thermally pre-stressed.

The transient dynamic stresses exceeds the design stress by about (50 %).

At ply orientation 35/-35/35 the natural frequency lowest by a .factor (9%) and (22%) for cone angle 55o and 75o respectively.

The transient dynamic stresses exceeds the design stress by about (50 %).

At ply orientation 35/-35/35 the natural frequency lowest by a factor (9%) and (22%) for cone angle 55^{o} and 75^{o} respectively.

The higher circumferential wave number, the more pronounced is the influence of ply orientation on the resulting natural frequency.

The ratio of ωmax/ωmin for cone angle 35o and different ply orientation are (6.67 for 0/90/0, 4.44 for 35/-35/35, 3.89 for 55/-55/55 and 3.33 for 75/-75/5-75).

The natural frequency drops appreciably (by about 18 %) as the temperature change from (20 ^{o}C) to

(300 ^{o}C) for axi-symmetrical mode shape.

References

[1] Dhotarad , M. S. and Gonesan , N. "Vibration Analysis of a Rectangular Plate Subjected to a Thermal Gradient" , J. of Sound and Vibration , Vol.60, N0.4 , PP.481-497 , 1978.

[2] Fauconneau , G. and Marangoni , R. D. ,"Effect of a Thermal Gradient on the Natural Frequencies of a Rectangular Plate ", Int. J. of Mechanical Science , Vol.12 , PP.113-122 , 1970.

[3] Ross, C.T.F., FINITE ELEMENT PROGRAMS FOR AXISYMMETRIC PROBLEMS IN ENGINEERING, Ellis Horwood Publishers, 1984.

[4] Ross, C. T. F. ,"Finite Elements for the Vibration of Cones and Cylinders" ,Int. J. for Numerical Methods in Engineering , Vol.9,PP.833-845,1975.

[5] Irons B. and Ahmad S., TECHNIQUES OF FINITE ELEMENTS, Gllis Horwood Publishers, 1980.

[6] Novozhilov V. V., THE THEORY OF THIN SHELLS, P. Noordhoff Ltd., 1959.

[7] Leissa A. W., "Shock and Vibration", Digest 13, 19-36.

[8] "Structural Alloys Handbook", Mechanical Properties ,Data Center, Columbus Laboratories ,1985.

NOTATIONS

Symbols	*Definition*	Units
[A]	Extensional Stiffness Matrix	
[B]	Coupling Stiffness Matrix	
$[B_E]$	Extensional Strain Displacement Matrix	
$[B_B]$	Bending Strain Displacement Matrix	
[D]	Bending Stiffness Matrix	
[DC]	Transformation Matrix	
E	Young's Modulus of Elasticity	$[N/mm^2]$
E_1	Young's Modulus in 1-axis Direction	$[N/mm^2]$
E_2	Young's Modulus in 2-axis Direction	$[N/mm^2]$
G_{12}	Shear Modulus in 1-2 Plane	$[N/mm^2]$
[K]	System Stiffness Matrix	
[k]	Element Stiffness Matrix	
[M]	System Mass Matrix	
[m]	Element Mass Matrix	
T(x,z)	Temperature Distribution	$[C^o]$
T_1	Temperature at ξ=-1	$[C^o]$
T_2	Temperature at ξ=+1	$[C^o]$
T	Thickness of Shell	[mm]
V_f	fiber Volume Fraction	
U,V	Auxiliary Variable	
$V_{o\{A,B,D\}}$,$V_{1\{A,B,D\}}$ $V_{2\{A,B,D\}}$,$V_{3\{A,B,D\}}$ $V_{4\{A,B,D\}}$	Invariant Transformed Stiffness	
u,v,w	Displacement in x,y,z Direction Respectively	[mm]
{u}	Nodal Displacement Vector	
$\overline{w}$	Displacement Vector	[mm]
X,Y,Z	Pressure Components in x,y,z Direction	$[N/mm^2]$
Y	Argument for Thomson's Function in Conical Part	
{ε}	Strain Vector	
$\{\varepsilon_E\}$	Elastic Strain	
$\{\varepsilon_T\}$	Thermal Strain	
ζ , η	Complex Argument	
x , μ	Auxiliary Constant	
∂	Partial Derivative	
θ	Fiber Orientation Angle	^{o}
ϕ	Cone Angle	^{o}
ρ	Density	$[Kg/mm^3]$
ξ	Intrinsic Coordinate	
υ	Poisson's Ratio	
Δ	Incremental Value	
γ	Shear Strain	
φ	Response Surface Operator	
Ψ	weight percent of glass	
Ω	Volume Domain	
ε_ϕ	Meridional Strain	
ε_θ	Hoop Strain	
ε_x	Axial Strain	
ω	Natural Frequency	[rad/s]

Table (1) Comparison of Natural Frequency

	Zimer – D	ANSYS	Expermental
Natural Frequency (Hz) Lobe No. (2)	970	980	978
Natural Frequency (Hz) Lobe No. (3)	890	903	902

Table (2) Dynamic Convergence Study

No. of Elements	No. of Nodes	No. of D.O.F.	ω (Hz)
12	13	12	25
16	17	16	26
19	20	19	54
29	30	29	87
37	38	37	91
50	49	48	88

Table (3) Variation of Natural Frequency with Lobe No. (Thickness=0.5 mm)

Lobe No.	$W_{1\ (Mat.\ 1)}$	$W_{2\ (Mat.1)}$	$W_{3(Mat.1)}$	$W_{1(Mat.2)}$	$W_{2(Mat.2)}$	$W_{3(Mat.2)}$
0	87.90	393.06	556.43	79.77	356.34	504.45
1	2.17	14.47	39.74	1.969	13.11	36.03
2	9.27	15.14	27.95	8.41	13.72	25.34
3	24.44	25.36	28.47	22.15	22.99	25.81
4	46.73	47.10	48.07	42.35	42.70	43.58
5	75.54	75.96	76.74	68.48	68.86	69.57

Table (4) Variation of Natural Frequency with Lobe No. (Thickness=0.7 mm)

Lobe No.	*w1 (Mat. 1)*	*w2 (Mat.1)*	*w3 (Mat.1)*	*w1 (Mat.2)*	*w2 (Mat.2)*	*w3 (Mat.2)*
0	85.05	392.2	556.31	77.11	355.56	504.34
1	2.17	14.47	39.75	1.97	13.12	36.04
2	12.56	17.41	29.32	11.38	15.78	26.58
3	34.17	34.96	37.49	30.98	31.70	33.99
4	65.40	65.86	66.87	59.29	59.71	60.63
5	105.78	106.46	107.68	95.90	96.54	97.62

Table (5) Variation of Natural Frequency with Lobe No. (Thickness=1.0 mm)

Lobe No.	*w1 (Mat. 1)*	*w2 (Mat.1)*	*w3 (Mat.1)*	*w1 (Mat.2)*	*w2 (Mat.2)*	*w3 (Mat.2)*
0	80.60	390.91	556.07	73.07	354.39	504.12
1	2.17	14.47	39.76	1.97	13.12	36.04
2	17.61	21.46	32.65	15.96	19.45	29.05
3	48.78	49.54	51.68	44.23	44.91	46.85
4	93.43	94.68	95.33	84.70	85.29	86.43
5	151.15	152.39	154.40	137.02	138.15	139.98

Table (6) Variation of Modulus of Elasticity and Natural Frequency With Temperature(Thick.=0.5 mm ,n=0)

$T(C^o)$	$E_{(Mat.1)}$(MPa)	$\omega_{1(Mat.1)}$(Hz)	$E_{(Mat.2)}$(MPa)	$\omega_{1(Mat.2)}$(Hz)
0	210000	87.60	175000	80.32
100	205800	87.10	171500	79.51
200	199000	85.65	166250	78.29
300	189000	83.47	157500	76.20
500	147000	73.61	122500	67.20

Table (7) Variation of Modulus of Elasticity and Natural Frequency With Temperature(Thick.=0.5 mm ,n=0)

Temp. Co	ω1 (Mat. 1)	ω2 (Mat.1)	ω3 (Mat.1)	ω1 (Mat.2)	ω2 (Mat.2)	ω3 (Mat.2)
0	133.01	399.65	563.21	121.48	364.32	514.41
50	121.02	397.23	561.01	113.97	362.94	512.81
100	108.60	395.03	558.60	105.29	361.52	511.08
150	93.41	393.11	556.69	95.54	360.12	509.30
200	76.75	391.45	553.82	84.88	358.81	507.58
250	57.43	389.66	548.30	73.46	357.65	506.00
300	42.65	389.82	551.78	61.19	356.61	504.39

Table (8) Variation of Modulus of Elasticity and Natural Frequency With Temperature(Thick.=0.5 mm ,n=1)

Temp. Co	ω1 (Mat. 1)	ω2 (Mat.1)	ω3 (Mat.1)	ω1 (Mat.2)	ω2 (Mat.2)	ω3 (Mat.2)
0	10.06	32.01	63.12	9.14	29.24	57.62
50	9.96	31.69	63.60	9.11	29.19	57.54
100	9.91	31.88	62.88	9.07	29.14	57.46
150	9.85	31.80	62.74	9.03	29.08	57.37
200	9.79	31.71	62.58	8.99	29.03	57.27
250	9.69	31.50	62.12	8.95	28.96	57.17
300	9.69	31.57	62.37	8.90	28.89	57.01

Table (9) Variation of Modulus of Elasticity and Natural Frequency With Temperature(Thick.=0.5 mm ,n=2)

Temp. Co	ω1 (Mat. 1)	ω2 (Mat.1)	ω3 (Mat.1)	ω1 (Mat.2)	ω2 (Mat.2)	ω3 (Mat.2)
0	9.27	15.14	27.95	8.46	13.82	25.51
50	9.22	15.06	27.80	8.42	13.73	25.41
100	9.10	14.87	27.64	8.39	13.46	25.30
150	9.16	14.74	27.48	8.35	13.54	25.19
200	9.05	14.66	27.33	8.31	13.45	25.09
250	8.99	14.47	27.15	8.27	13.36	24.98
300	8.93	14.33	27.61	8.23	13.26	24.87

Table (10) Variation of Modulus of Elasticity and Natural Frequency With Temperature(Thick.=0.5 mm ,n=3)

Temp. Co	ω1 (Mat. 1)	ω2 (Mat.1)	ω3 (Mat.1)	ω1 (Mat.2)	ω2 (Mat.2)	ω3 (Mat.2)
0	22.31	23.15	25.99	24.44	25.36	28.47
50	22.29	23.08	25.87	24.41	25.27	28.29
100	22.27	23.02	25.74	24.38	25.17	28.16
150	22.25	22.96	25.62	24.36	25.68	27.93
200	22.23	22.89	25.49	24.33	24.98	27.75
250	22.21	22.83	25.36	24.30	24.89	27.56
300	22.19	22.76	25.24	24.27	24.80	27.38

Table (11) Variation of Modulus of Elasticity and Natural Frequency With Temperature(Thick.=0.5 mm ,n=4)

Temp. Co	ω1 (Mat. 1)	ω2 (Mat.1)	ω3 (Mat.1)	ω1 (Mat.2)	ω2 (Mat.2)	ω3 (Mat.2)
0	46.17	47.1	48.07	42.65	42.99	43.88
50	46.07	47.04	47.93	42.64	42.95	43.80
100	46.68	46.98	47.83	42.62	42.91	43.71
150	46.66	46.92	47.70	42.61	42.87	43.63
200	46.61	46.86	47.58	42.60	42.83	43.54
250	46.60	46.80	46.46	42.58	42.79	43.46
300	46.51	46.75	47.34	42.56	42.74	43.37

Table (12) Variation of Modulus of Elasticity and Natural Frequency With Temperature(Thick.=0.5 mm ,n=5)

Temp. Co	ω1 (Mat. 1)	ω2 (Mat.1)	ω3 (Mat.1)	ω1 (Mat.2)	ω2 (Mat.2)	ω3 (Mat.2)
0	75.54	75.96	76.74	68.96	69.34	70.06
50	75.53	75.92	76.66	68.95	69.31	70.00
100	75.51	75.88	76.58	68.94	69.28	69.94
150	75.50	75.83	76.49	68.93	69.25	69.88
200	75.48	75.79	76.41	68.92	69.22	69.82
250	75.46	75.74	76.32	68.91	69.19	69.76
300	75.43	75.69	76.24	68.89	69.16	69.71

Table (13) The Material Properties of the Composite Materials

Property	Material 1	Material 2	Material 3
E_1 (GPa)	36.500	142.000	72000
E_2 (GPa)	8.5000	10.3000	72000
G_{12} (GPa)	3.1450	7.2000	72000
ν_{12}	0.2830	0.2700	0.3
α_1 ($1/^oC$)$\times 10^{-6}$	11.000	-0.9000	11.7
α_2 ($1/^oC$) $\times 10^{-6}$	23.000	27.000	11.7
ρ (Kg/m^3)	1930.0	1580.0	2700

Table (14) Variation of Natural Frequency with Lobe No. for Material 1

Ply Angle	Lobe No	Cone Angle								
		f = 35º			f = 55º			f = 75º		
		w_1 (Hz)	w_2 (Hz)	w_3 (Hz)	w_1 (Hz)	w_2 (Hz)	w_3 (Hz)	w_1 (Hz)	w_2 (Hz)	w_3 (Hz)
0/90/0	0	121.4	145.9	214.8	-	-	-	-	-	-
	1	17.22	55.15	103.5	16.49	52.85	100.2	15.65	50.33	96.30
	2	26.65	58.18	90.26	24.69	38.83	60.43	13.47	28.38	58.37
	3	29.02	48.58	74.32	28.79	48.05	73.46	28.00	38.42	48.37
	4	46.46	57.32	76.10	46.37	57.04	75.63	46.12	56.00	70.78
	5	72.56	79.64	93.35	72.51	79.46	92.99	72.36	78.85	91.48
35/-35/35	0	76.89	122.9	157.8	69.28	85.60	137.9	58.65	69.4	148.6
	1	16.70	75.13	137.9	15.79	70.79	136.8	14.79	66.76	135.8
	2	30.29	74.32	107.7	26.50	41.33	79.29	12.87	31.97	76.04
	3	32.31	58.92	97.40	31.91	57.40	88.95	30.24	38.81	57.33
	4	52.45	67.76	94.94	52.28	67.10	93.65	51.72	63.94	73.40
	5	81.61	93.50	114.2	81.49	93.05	113.3	81.11	91.42	107.7
55/-55/55	0	62.93	128.5	184.5	55.09	82.05	152.6	50.95	60.42	164.7
	1	13.83	64.87	144.1	13.02	60.88	138.5	12.14	56.91	132.2
	2	27.04	67.15	104.3	24.87	41.31	70.77	14.07	27.98	66.02
	3	38.33	57.13	90.62	38.07	55.96	86.96	37.12	43.51	55.72
	4	68.01	78.32	98.30	67.88	77.83	97.17	67.54	76.04	85.26
	5	107.9	116.3	131.3	107.8	116.0	130.5	107.5	114.9	127.6
75/-75/75	0	71.61	142.2	196.1	57.43	60.75	230.1	43.99	52.53	252.2
	1	13.17	52.83	114.0	12.44	50.12	108.2	11.63	47.24	102.2
	2	26.16	57.42	92.66	25.13	48.62	63.62	18.92	27.66	56.31
	3	44.80	56.90	79.55	44.68	56.31	78.20	44.38	54.02	61.90
	4	82.51	88.01	99.73	82.46	87.79	99.22	82.34	87.20	97.50
	5	132.4	136.4	144.2	132.3	136.2	143.9	132.3	135.9	142.9

Table (15) Variation of Natural Frequency with Lobe No. for Material 2

Ply Angle	Lobe No	Cone Angle								
		f = 35°			f = 55°			f = 75°		
		w_1 (Hz)	w_2 (Hz)	w_3 (Hz)	w_1 (Hz)	w_2 (Hz)	w_3 (Hz)	w_1 (Hz)	w_2 (Hz)	w_3 (Hz)
0/90/0	0	244.0	-	-	82.71	-	-	60.09	-	-
	1	31.16	97.05	177.7	29.95	93.28	172.3	28.54	89.02	165.6
	2	46.85	102.1	158.8	42.07	61.36	104.9	21.14	89.02	102.4
	3	45.52	83.22	130.5	45.10	82.42	129.0	43.22	57.03	81.84
	4	66.76	90.00	127.7	66.58	89.51	126.9	66.05	87.37	104.7
	5	101.8	117.2	146.6	101.7	116.9	145.9	101.4	115.7	142.8
35/-35/35	0	132.3	198.3	245.8	124.4	169.5	218.6	114.6	129.5	231.8
	1	31.81	150.5	245.8	30.04	141.4	247.3	28.12	133.6	249.8
	2	58.50	143.4	198.0	45.00	69.91	156.2	19.27	61.37	151.4
	3	58.61	114.8	193.7	57.64	110.2	141.8	48.94	61.87	110.0
	4	91.86	126.1	184.8	91.42	124.5	181.5	88.94	101.5	124.2
	5	141.1	168.9	215.3	140.8	167.8	213.0	139.4	157.9	171.2
55/-55/55	0	94.79	213.2	307.1	84.09	166.6	248.0	78.08	123.5	262.3
	1	21.98	111.4	265.6	20.67	104.0	253.9	19.24	96.79	240.8
	2	47.40	117.9	188.9	43.63	69.62	123.1	24.53	48.30	114.1
	3	76.50	107.4	167.1	76.04	105.2	159.6	72.29	78.46	103.7
	4	138.0	156.8	192.2	137.8	155.8	189.9	136.9	146.7	156.1
	5	219.5	236.1	264.5	219.3	235.3	262.8	218.7	232.3	243.1
75/-75/75	0	92.09	241.5	351.2	74.50	111.5	404.7	66.83	82.75	432.5
	1	17.60	80.82	184.3	16.57	76.27	173.4	15.44	71.40	162.5
	2	44.40	90.61	151.1	43.25	83.15	112.9	38.08	71.40	87.50
	3	93.64	107.7	139.2	93.51	106.9	137.0	93.20	104.8	123.8
	4	176.1	183.1	198.2	176.0	182.8	197.4	175.9	182.0	195.2
	5	283.6	289.4	300.3	283.5	289.1	299.8	283.4	288.6	298.4

Table (16) Variation of Natural Frequency with Lobe No. for Material 3

Ply Angle	Lobe No	Cone Angle								
		f = 35°			f = 55°			f = 75°		
		w_1 (Hz)	w_2 (Hz)	w_3 (Hz)	w_1 (Hz)	w_2 (Hz)	w_3 (Hz)	w_1 (Hz)	w_2 (Hz)	w_3 (Hz)
Isotropic	0	165.3	302.3	366.1	124.0	141.6	346.6	90.15	129.5	383.2
	1	30.96	117.1	234.7	29.33	111.2	226.4	27.52	105.2	217.5
	2	52.88	122.1	188.0	49.42	87.77	130.0	30.13	56.52	122.3
	3	64.33	101.5	156.8	63.87	99.90	153.5	62.56	87.59	104.2
	4	110.1	128.9	164.5	109.9	128.2	163.1	109.5	126.0	155.9
	5	174.3	187.4	212.3	174.2	186.9	211.3	173.8	185.6	208.0

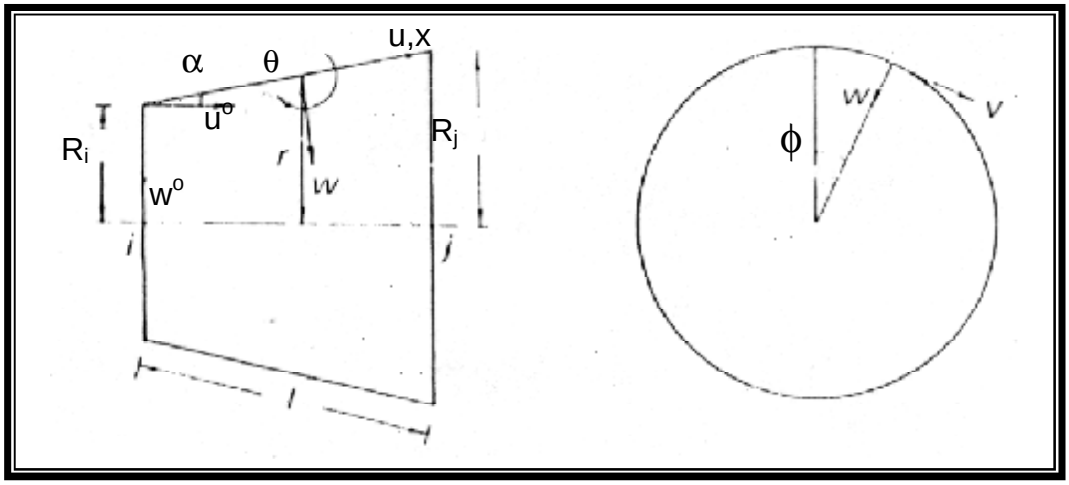

Fig. (1) Truncated Conical Shell Element [4]

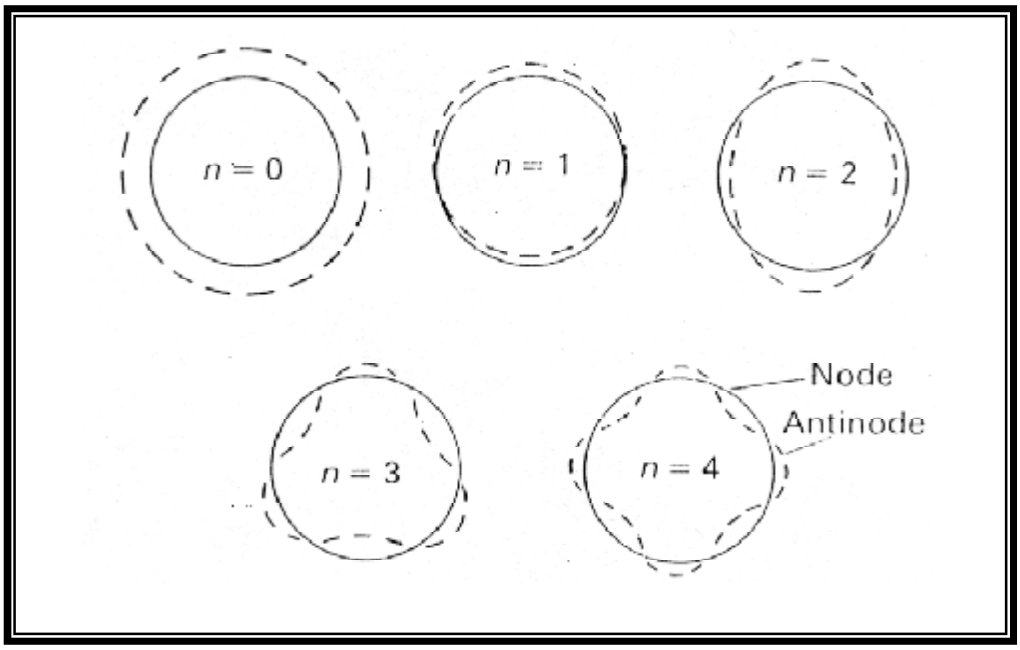

Fig. (2) Circumferential Wave Patterns [4]

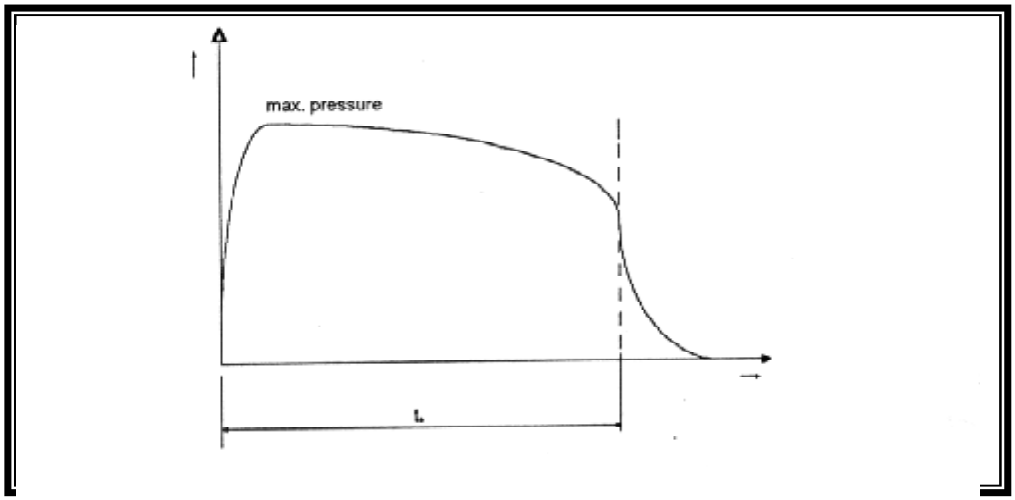

Fig(3) Pressure Time Curve for Solid Propellant Rocket Motor

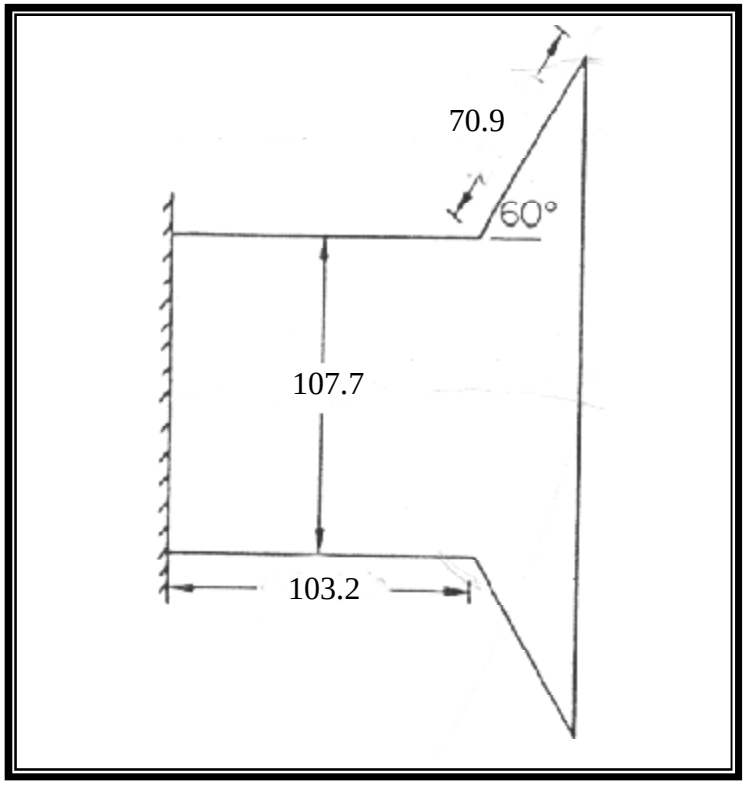

$E=4.4816\times10^{4}$ MPa
$\nu = 0.3$
$\rho=1.69913\times10^{-9}$ Kg/mm^3
$t_{cone}=2.64$ mm
$t_{cyl}=6.40$ mm
All Dimensions in mm

Fig. (4) Conical – Cylindrical Intersection [4]

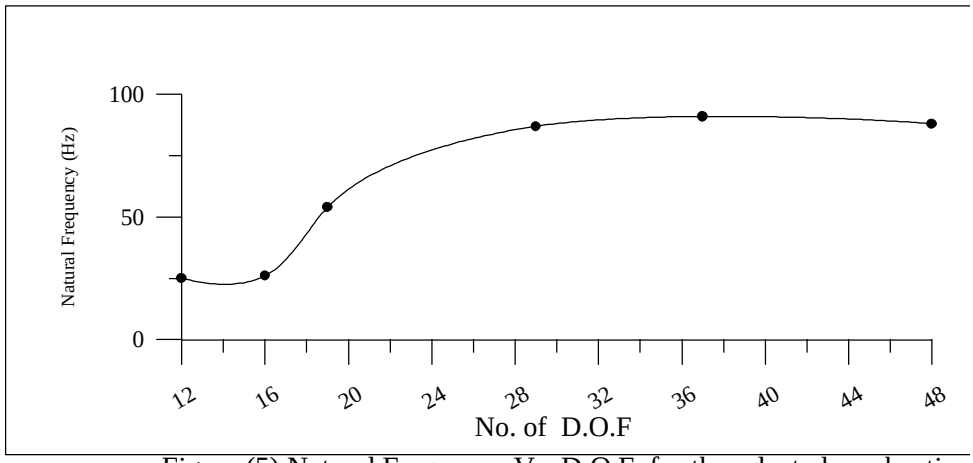

Figure (5) Natural Frequency Vs. D.O.F. for the selected combustion chamber Combustion Chamber Case

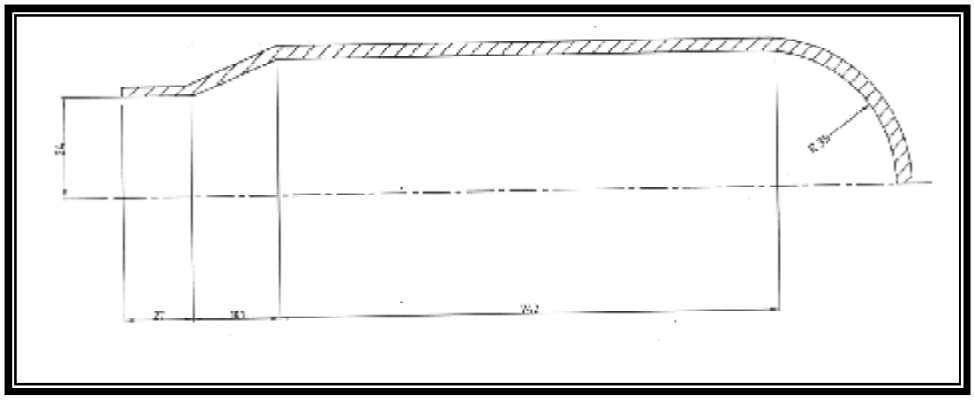

	Specification	E(MPa)	α	υ	ρ(Kg/mm^3)
Material (1)	D6AC	210000	13.32×10^{-6}	0.3	7.9×10^{-6}
Material (2)	18NiMarage300	175000	10.08×10^{-6}	0.3	8.0×10^{-6}

Figure (6) A Real Case of Rocket Combustion Chamber

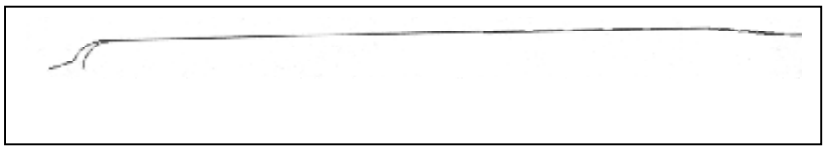

Figure(7) Vibration Mode of Rocket Combustion Chamber Case
(ω_1=87.90 Hz , Lobe No.=0)

Figure(8) Vibration Mode of Rocket Combustion Chamber Case
(ω2=393.06 Hz , Lobe No.=0)

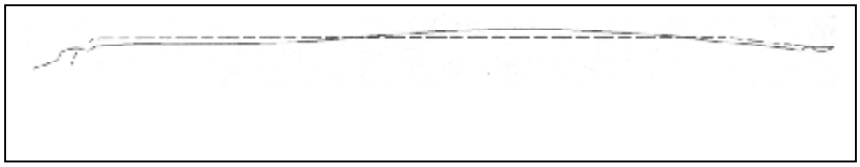

Figure(9) Vibration Mode of Rocket Combustion Chamber
(ω3=556.43 Hz , Lobe No.=0)

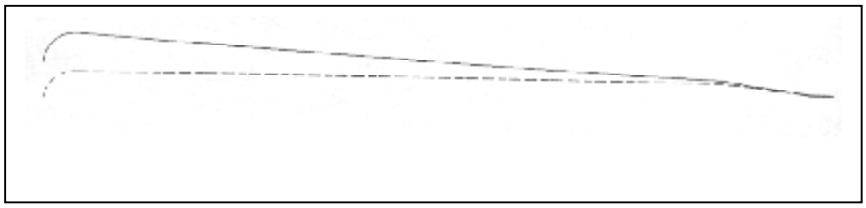

Figure(10) Vibration Mode of Rocket Combustion Chamber Case
(ω1=2.17 Hz , Lobe No.=1)

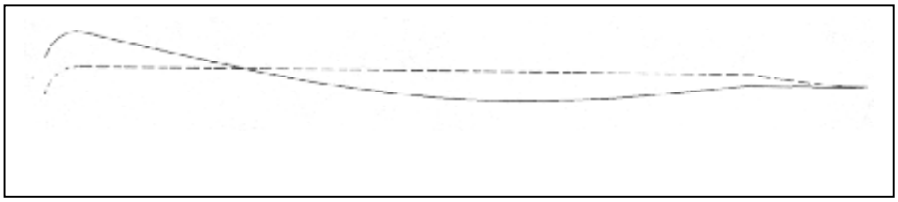

Figure(11) Vibration Mode of Rocket Combustion Chamber Case
(ω2=14.47 Hz , Lobe No.=1)

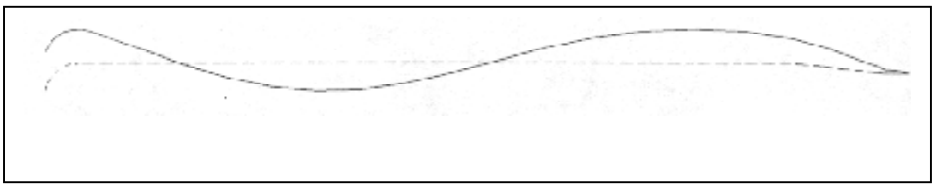

Figure(12) Vibration Mode Rocket Combustion Chamber Case
(ω3=39.75 Hz , Lobe No.=1)

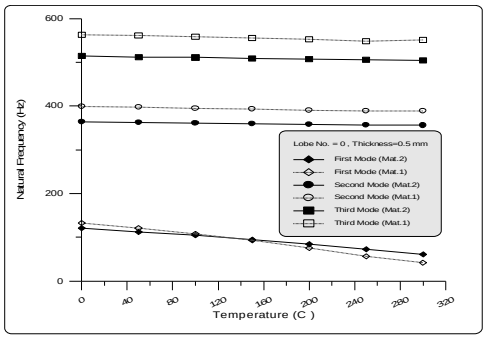

Fig.(13) Natural Frequency Vs. Temperature

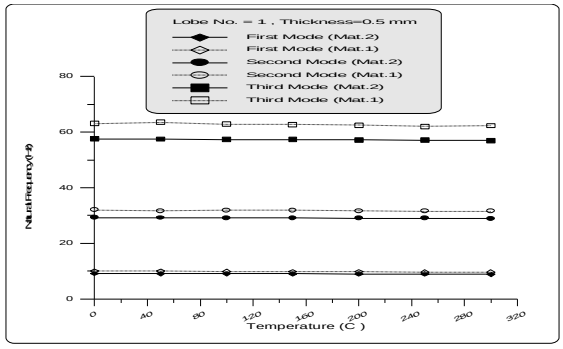

Fig.(14) Natural Frequency Vs. Temperature

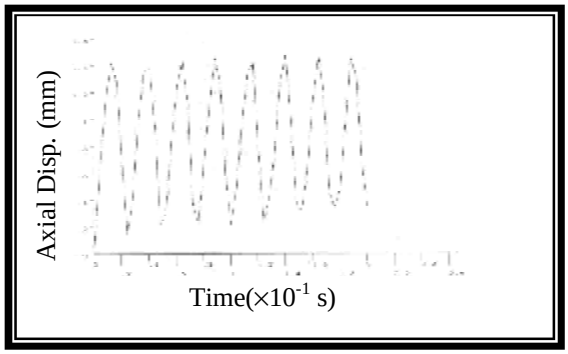

Figure (15) Displacement History For Rocket Combustion Chamber Case (Damping Ratio = 0)

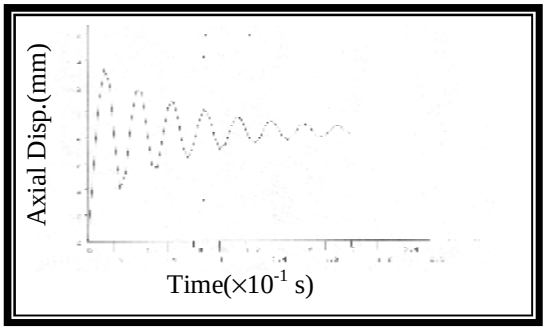

Figure (16) Displacement History For Rocket Combustion Chamber Case (Damping Ratio = 0.0005)

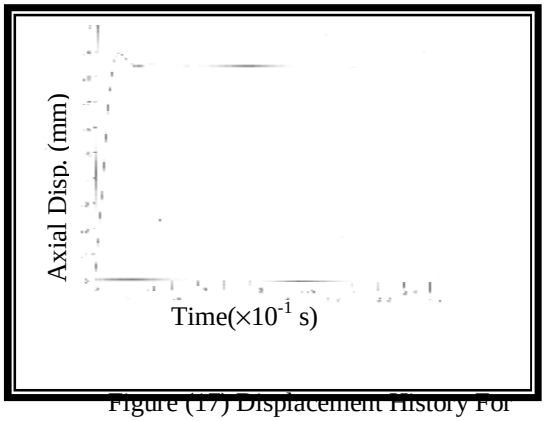

Figure (17) Displacement History For Combustion Chamber Case (Damping Ratio = 0.005)

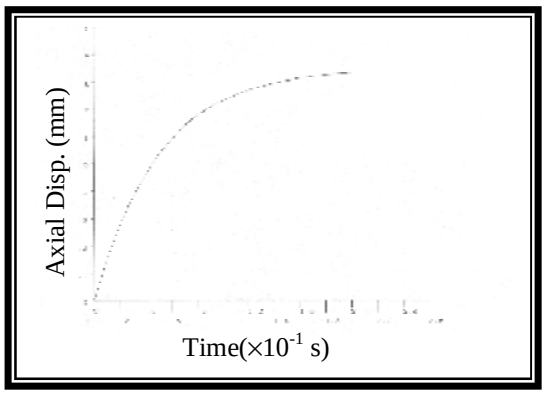

Figure (18) Displacement History For Rocket Combustion Chamber Case (Damping Ratio = 0. 05

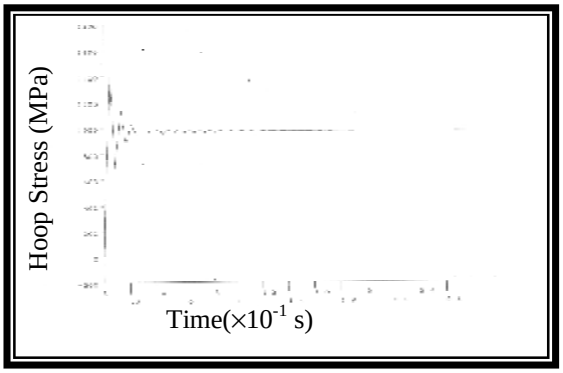

Figure (19) Hoop Stress History For Rocket Combustion Chamber Case

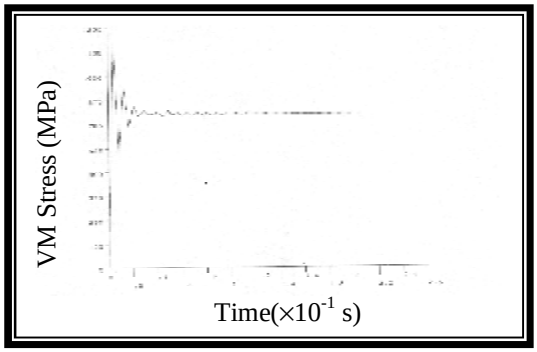

Figure (20) Hoop Stress History For Rocket Combustion Chamber Case

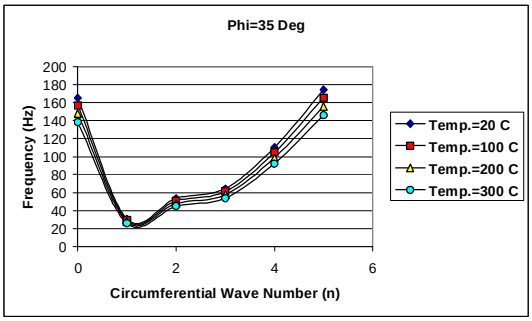

Fig.(21) Frequency Vs. Circumferential Wave No. for Cylindrical – Conical Shell

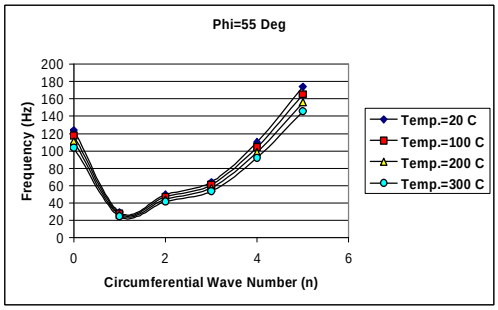

Fig.(22) Frequency Vs. Circumferential Wave No. for Cylindrical – Conical Shell

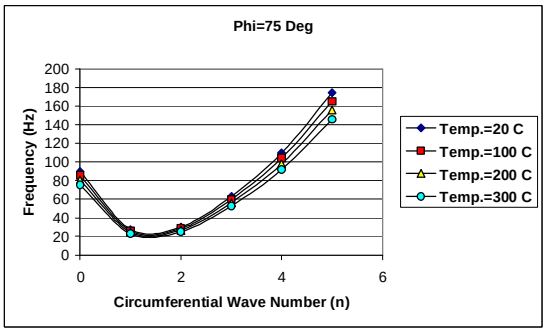

Fig.(23) Frequency Vs. Circumferential Wave No. for Cylindrical – Conical Shell

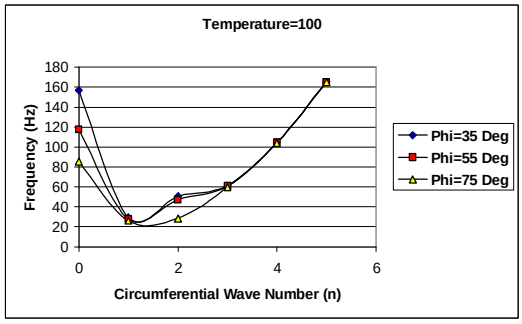

Fig.(24) Frequency Vs. Circumferential Wave No. for Cylindrical – Conical Shell

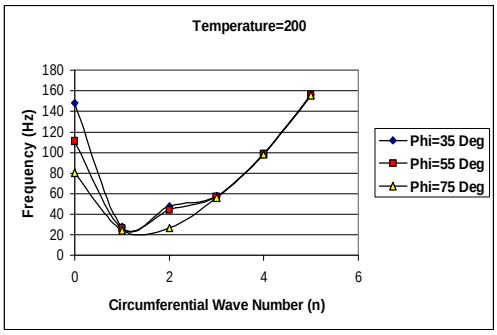

Fig.(25) Frequency Vs. Circumferential Wave No. for Cylindrical – Conical Shell

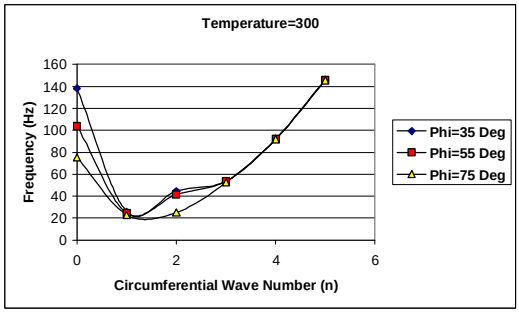

Fig.(26) Frequency Vs. Circumferential Wave No. for Cylindrical – Conical Shell